Teacher Guided Architecture Search

Pouya Bashivan
Department of Brain and Cognitive Sciences
McGovern Institute for Brain Research
MIT

bashivan@mit.edu

Mark Tensen
University of Amsterdam
mark.tensen@student.uva.nl

James J DiCarlo
Department of Brain and Cognitive Sciences and
McGovern Institute for Brain Research
MIT

dicarlo@mit.edu

Abstract

Much of the recent improvement in neural networks for computer vision has resulted from discovery of new networks architectures. Most prior work has used the performance of candidate models following limited training to automatically guide the search in a feasible way. Could further gains in computational efficiency be achieved by guiding the search via measurements of a high performing network with unknown detailed architecture (e.g. the primate visual system)? As one step toward this goal, we use representational similarity analysis to evaluate the similarity of internal activations of candidate networks with those of a (fixed, high performing) teacher network. We show that adopting this evaluation metric could produce up to an order of magnitude in search efficiency over performance-guided methods. Our approach finds a convolutional cell structure with similar performance as was previously found using other methods but at a total computational cost that is two orders of magnitude lower than Neural Architecture Search (NAS) and more than four times lower than progressive neural architecture search (PNAS). We further show that measurements from only ~300 neurons from primate visual system provides enough signal to find a network with an Imagenet top-1 error that is significantly lower than that achieved by performance-guided architecture search alone. These results suggest that representational matching can be used to accelerate network architecture search in cases where one has access to some or all of the internal representations of a teacher network of interest, such as the brain's sensory processing networks.

1. Introduction

The accuracy of deep convolutional neural networks (CNNs) for visual categorization has advanced substantially from 2012 levels (AlexNet [25]) to current state-of-the-art CNNs like ResNet [19], Inception [41], DenseNet [21]. This progress is mostly due to discovery of new network architectures. Yet, even the space of feedforward neural network architectures is essentially infinite and given this complexity, the design of better architectures remains a challenging and time consuming task.

Many approaches have been proposed in recent years to automate the discovery of neural network architectures, including random search [32], reinforcement learning [44, 45], evolution [37, 36], and sequential model based optimization (SMBO) [28, 8]. These methods operate by iteratively sampling from the hyperparameter space, training the corresponding architecture, evaluating it on a validation set, and using the search history of those scores to guide further architecture sampling. But even with recent improvements in search efficiency, the total cost of architecture search is still outside the reach of many groups and thus impedes the research in this area (e.g. some of the recent work in this area has spent more than 20k GPU-hours for each search experiment [36, 44]).

What drives the total computational cost of running a search? For current architectural search procedures (above), the parameters of each sampled architecture must be trained before its performance can be evaluated and the amount of such training turns out to be a key driver in the total computational cost. Thus, to reduce that total cost, each architecture is typically only partially trained to a *premature* state and its *premature* performance is used as a proxy of

its *mature* performance (i.e. the performance it would have achieved if was actually fully trained).

Because the search goal is high *mature* performance in a task of interest, the most natural choice of an architecture evaluation score is its *premature* performance. However, this may not be the best choice of evaluation score. For example, it has been observed that, as a network is trained, multiple sets of internal features begin to emerge over network layers, and the quality of these internal features determines the ultimate behavioral performance of the neural network as a whole. Based on these observations, we reasoned that, if we could evaluate the quality of a network's internal features even in a very *premature* state, we might be able to more quickly determine if a given architecture is likely to obtain high levels of *mature* performance.

But without a reference set of high quality internal features, how can we determine the quality of a network's internal features? The main idea proposed here is to use features of a high performing "teacher" network as a reference to identify promising sample architectures at a much earlier *premature* state. Our proposed method is inspired by prior work showing that the internal representations of a high-performing *teacher* network can be used to optimize the parameters of smaller, shallower, or thinner student networks [3, 20, 38, 13]. It is also inspired by the fact that such internal representation measures can potentially be obtained from primate brains and thus could be used as an ultimate teacher. While our ability to simultaneously record from large populations of neurons is fast growing [40], these measurements have already been shown to have remarkable similarities to internal activations of CNNs [43, 39].

One challenge in comparing representations across models or between models and brains is the lack of one-to-one mapping between the features (or neurons in the brain). Representational Similarity Analysis (RSA) is a tool that summarizes the representational behavior into a matrix called Representational Dissimilarity Matrix (RDM) that embeds the distance between activation in response to different inputs. In doing so it abstracts away from individual features (i.e. activations) and therefore enables us to compare the representations originating from different models or even between models and biological organisms.

Based on the RDM metric, we propose a method for architecture search termed "Teacher Guided Search for Architectures by Generation and Evaluation" (TG-SAGE). Specifically, TG-SAGE guides each step of an architecture search by evaluating the similarity between representations in the candidate network and those in a fixed, high-performing teacher network with unknown architectural parameters but observable internal states. We found that when this evaluation is combined with the usual performance evaluation (above), we can predict the mature performance of sampled architectures with an order of magnitude less

premature training and thus an order of magnitude less total computational cost. We then used this observation to execute multiple runs of TG-SAGE for different architecture search spaces to confirm that TG-SAGE can indeed discover network architectures of comparable mature performance to those discovered with performance-only search methods, but with far less total computational cost. More importantly, when considering the primate visual system as the teacher network with measurements of neural activity from only several hundred neural sites, TG-SAGE finds a network with an Imagenet top-1 error that was 5% lower than that achieved by performance-guided architecture search.

In section 2 we review some of the previous studies in neural networks architecture search and the use of RSA to compare artificial and biological neural networks. In section 3 we describe representational dissimilarity matrix and how we use this metric in TG-SAGE to compare representations. In section 4 we show the effectiveness of TG-SAGE in comparison to performance-guided search methods by using two search methods in different architectural spaces of increasing size. We then show that in the absence of a teacher model, how we can use measurements from the brain as a teacher to guide the architecture search.

2. Previous Work

There have been several recent studies on using reinforcement learning to design high performing neural network architectures [4, 44, 45]. Neural Architecture Search (NAS) [44, 45] utilizes a long short-term memory network (LSTM) trained using REINFORCE to learn to design neural network architectures for object recognition and natural language processing tasks. Real et al. [37, 36] used evolutionary approaches in which samples taken from a pool of networks were engaged in a pairwise competition game.

While most of these works have focused on discovering higher performing architectures, there has been a number of efforts emphasizing the computational efficiency in hyperparameter search. In order to reduce the computational cost of architecture search, Brock et al. [10] proposed to use a hypernetwork [18] to predict the layer weights for any arbitrary candidate architecture instead of retraining from random initial values. Hyperband [27] formulated hyperparameter search as a resource allocation problem and improved the efficiency by controlling the amount of resources (e.g. training) allocated to each sample. Similarly, several other methods proposed to increase the search efficiency by introducing early-stopping criteria during training [5] or by extrapolating the learning curve [14]. These approaches are closely related to our proposed method in that, their main focus is to reduce the per-sample training cost.

Several more recent methods [31, 29, 42, 1, 17] proposed to share the trainable parameters across all candidate net-

works and to jointly optimize for the hyperparameters and the network weights during the search. While these approaches led to significant reduction in total search cost, they can only be applied to the spaces of network architectures in which the number of trainable weights do not change as a result of hyperparameter choices (e.g. when the number of filters in a CNN is fixed).

On the other hand, there is a growing body of literature demonstrating the remarkable ability of deep neural networks trained on various categorization tasks in predicting neural and behavioral response patterns in primates. These models are able to predict the neural responses in parts of the primate visual [43, 12, 11] and auditory cortices [23], explain patterns of object similarity judgements [35, 22], shape sensitivity in primates [26], and even to control the neural activity in a mid-level visual cortical area [6]. Moreover, it has been shown that the categorization performance of deep artificial neural networks is strongly correlated with their ability to predict the neural responses along the ventral visual pathway [43, 2].

Nevertheless, while these networks have largely progressed our understanding of neural computations in many parts of the primate brain, there are still significant differences between the two [16, 34]. Inspired by these observations, some recent studies have utilized brain measurements as constraints to alter the artificial neural networks behavior to be more similar to the brain [15, 9].

3. Methods

3.1. Representational Dissimilarity Matrix

Representational Dissimilarity Matrix (RDM) [24] is an embedding computed for a representation that quantifies the dissimilarity between activation patterns in that representational space in response to a set of inputs or input categories. For a given input i, the n_a network activations at one layer can be represented as a vector $\vec{V} = f(i) \in \mathbb{R}^{n_a}$. Similarly, the collection of activations in response to a set of n_i inputs can be represented in a matrix $F \in \mathbb{R}^{n_i \times n_a}$ which contains n_a activations measured in response to n_i inputs.

For a given activation matrix F, we derive RDM (M^F) by computing the pairwise distances between each pair of activation vectors (i.e. F_i and F_j which correspond to rows i and j in activation matrix F) using a distance measure like the correlation residual.

$$M^F \in \mathbb{R}^{n_i \times n_i}, M_{i,j}^F = 1 - corr(F_i, F_j) \qquad (1)$$

When calculating RDM for different categories (instead of individual inputs) we substitute the matrix F with F^c in which each row c contains the average activation pattern across all inputs in category c.

RDM constitutes an embedding of the representational space that abstracts away from individual activations. Because of this, it allows us to compare the representations in different models or even between models and biological organisms [43, 12]. Once RDM is calculated for two representational spaces (e.g. for a layer in each of the student and teacher networks), we can evaluate the similarity of those representations by calculating the correlation coefficient (e.g. Pearson's r) between the values in the upper triangle of the two RDM matrices.

3.2. Teacher Representational Similarity as Performance Surrogate

The largest portion of cost associated with neural network architecture search comes from training the sampled networks, which is proportional to the number of training steps (SGD updates) performed on the network. Due to the high cost of fully training each sampled network, in most cases a surrogate score is used as a proxy for the *mature* performance. Correlation between the surrogate and *mature* score may affect the architecture search performance as poor proxy values could guide the search algorithm towards suboptimal regions of the space. Previous work on architecture search in the space of Convolutional Neural Networks (CNN) have concurred with the empirical surrogate measure of *premature* performance after about 20 epochs of training. While 20 epochs is much lower than the usual number of epochs used to fully train a CNN network (300-900 epochs), it still forces a large cost on conducing architecture searches. We propose that evaluating the internal representations of a network would be a more reliable measure of architecture quality during the early phase of training (e.g. after several hundreds of SGD iterations), when the features are starting to be formed but the network is not yet performing reliably on the task.

An overview of the procedure is illustrated in Figure-1. We evaluate each sampled candidate model by measuring the similarity between its RDMs at different layers (e.g. M^{C1-C4}) to those extracted from the teacher network (e.g. M^{T1-T3}). To this end, we compute RDM for all layers in the network and then compute the correlation between all pairs of student and teacher RDMs. To score a candidate network against a given layer in the teacher network, we consider the highest RDM similarity to teacher layer calculated over all layers of the student network (i.e. $S_1 - S_3$; $S_i = max_j(corr(M^{Ti}, M^{Cj}))$).

We then construct an overall teacher similarity score by taking the mean of the RDM scores which we call "Teacher Guidance" (TG). Finally, we define the combined Performance and TG score (P+TG) which is formulated as weighted sum of *premature* performance and TG score in the form of $P + \alpha TG$. The combined score guides the architecture search to maximize performance as well as rep-
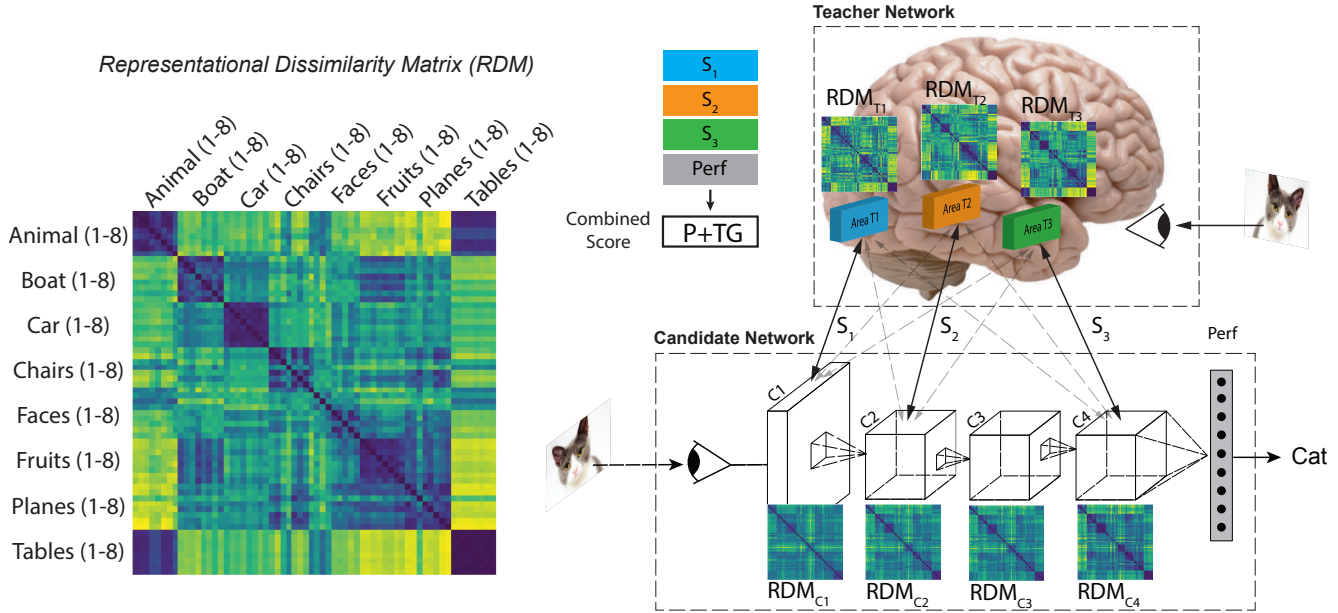
Figure 1. Left – Illustration of an exemplar RDM matrix for a dataset with 8 object categories and 8 object instances per category. Right – Overview of TG-SAGE method. Correlation between RDMs of candidate and teacher networks, are combined with candidate network premature performance to form P+TG score for guiding the architecture search.

resentational similarity with the teacher architecture. The α parameter can be used to tune the relative weight assigned to TG score compared to the performance score. We consider the teacher architecture as any high-performing network with unknown architecture but observable activations. We can have one or several measured endpoints from the teacher network that each could potentially be used to generate a similarity score.

4. Experiments and Results

4.1. Performance Predictability from Teacher Representational Similarity

We first investigated if the teacher similarity evaluation measure (P+TG) of premature networks improves the prediction of *mature* performance (compared to evaluation of only *premature* performance, P). To do this, we made a pool of CNN architectures for which we computed the *premature* and *mature* performances as well as the *premature* RDMs (a measure of the internal feature representation, see 3.1) at every model layer. To select the CNN architectures in the pool we first ran several performance-guided architecture searches with 20 epoch/sample training (see section 4.2 and supplementary material) and then selected 116 architectures found at different stages of the search. These networks had a wide range of *mature* performance levels that also included the best network architectures found during each search.

In experiments carried out in sections 4.1 to 4.3, we used a variant of ResNet [19] with 54 convolutional layers ($n=9$) as the teacher network. This architecture was selected as

the *teacher* because it is high performing (top-1 accuracy of 94.75% and 75.89% on CIFAR10 and CIFAR100 datasets respectively). Notably, the teacher architecture is not in our search spaces (see supp. material). Layer activations after each of the three stacks of residual blocks (here named L1-L3) were chosen as the teacher's internal feature maps. For each feature map, we took 10 random subsample of features, computed the RDM for each subsample, and then computed the average RDM across all subsamples. We did not attempt to optimize the choice of layers in the teacher network these were chosen simply because they sampled approximately evenly over the full depth of the teacher.

In order to find the optimum TG weight factor, we varied the α parameter and measured the change in correlation between the P+TG score and the mature performance (Figure 2). We observed that higher α led to larger gains in predicting the mature performance when models were trained only for few epochs (≤ 2.5 epochs). However, with more training, larger α values reduced the predictability. We found that for networks trained for ~ 2 epochs, a value of $\alpha = 1$ is close to optimum. The combined "P+TG" score (see 3.2) composes the best predictor of *mature* performance during most of the early training period (Figure 3-bottom). This observation was consistent with previous findings that learning in deep networks predominantly happen "bottom-up" [33].

We further found that the earlier teacher layers (L1) are better predictors of the *mature* performance compared to other layers early on during the training (<2epochs) but

as the training progresses, the later layers (L2 and L3) become better predictors ($\sim$3epochs) and with more training ($>$3epochs) the *premature* performance becomes the best single predictor of the *mature* (i.e. fully trained) performance (Figure 3).

In addition to ResNet, we also analyzed a second teacher network, namely NASNet (see section 2 in supp. material) and confirmed our findings using the alternative teacher network. We also found that NASNet activations (which performs higher than ResNet; 82.12% compared to 75.9%) form a better predictor of *mature* performance in almost all training regimes (see supp. material).
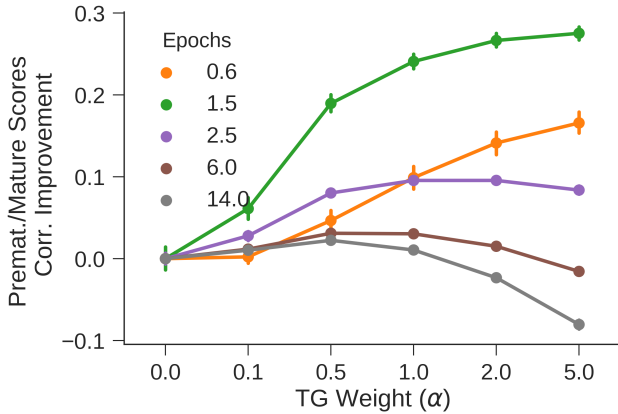

Figure 2. Effect of TG weight α on predicting the mature performance.

4.2. Teacher Guided Search in the Space of Convolutional Networks

As outlined in the Introduction, we expected that the (P+TG) evaluation score's improved predictivity (Figure 3) should enable it to support a more efficient architecture search than performance evaluation alone (P). To test this directly, we used the (P+TG) evaluation score in full architectural search experiments using a range of configurations. For these experiments, we searched two spaces of convolutional neural networks similar to previous search experiments [44] (maximum network depth of either 10 or 20 layers). These architectural search spaces are important and interesting because they are large. In addition, because networks in these search spaces are relatively inexpensive to train to maturity, we could evaluate the true underlying search progress at a range of checkpoints (below). We ran searches in each space using four different search methods: using the (P+TG) evaluation score at 2 or 20 epochs of premature training, and using the (P) evaluation score at either 2 or 20 epochs of premature training. For these experiments, we used random [32], reinforcement learning (RL) [44], as well as TPE architecture selection algorithm [7] (see Methods), and we halted the search after 1000 or

2000 sampled architectures (for the 10- and 20-layer search spaces, respectively). We conducted our search experiments on CIFAR100 instead of CIFAR10 because of larger number of classes in the dataset that provided a higher dimensional RDM.

We found that, for all search configurations, the (P+TG) driven search algorithm (i.e. TG-SAGE) consistently outperformed the performance-only driven algorithm (P) in that, using equal computational cost it always discovered higher performing networks (Table 1). This gain was substantial in that TG-SAGE found network architectures with approximately the same performance as (P) search but at $\sim 10\times$ less computational cost (2 vs. 20 epochs; Table 1).

To assess and track the efficiency of these searches, we measured the maximum validation set performance of the fully trained network architectures returned by each search at its current choice of the top-5 architectures. We repeated each search experiment three times to estimate variance in these measures resulting from both search sampling and
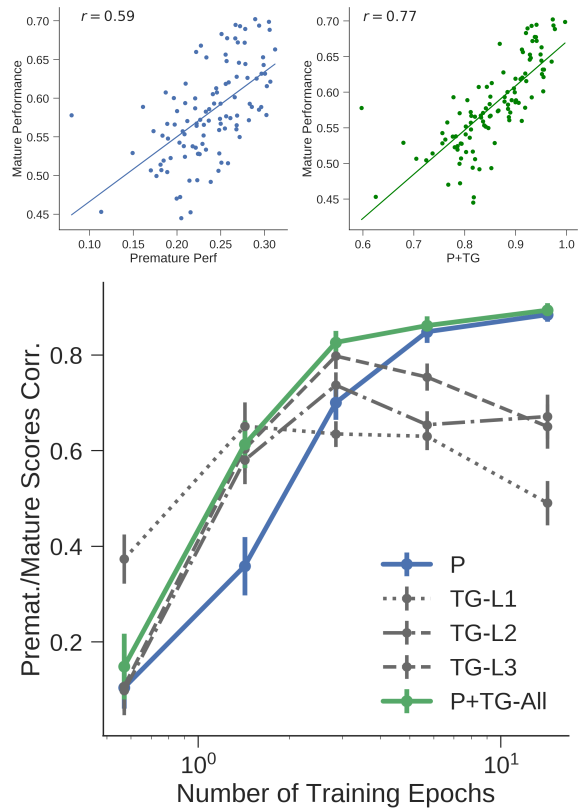

Figure 3. Comparison of performance and P+TG measures at premature state (epochs=2) as predictors of mature performance. (top-left) Scatter plot of premature and mature performance values. (top-right) Scatter plot of premature P+TG measure and mature performance. (bottom) Correlation between performance, single layer RDMs, and combined P+TG measures with mature performance at varying number of premature training epochs.

Table 1. Comparison of premature performance and representational similarity measure in architecture search using RL and TPE algorithms. P: premature performance as validation score; P+TG: combined premature performance and RDMs as the validation score. Values are $\mu \pm \sigma$ across 3 search runs.

Search Algorithm	RL				TPE	
Search Space	10 layer		20 layer		10 layer	20 layer
# Epoch/Sample	2	20	2	20	2	2
Random - Best C100 Error (%)	45.4± 2.5	41.3± 1.5	41.2± 1.8	38.3± 4.8	45.4± 2.5	41.2± 1.8
P - Best C100 Error (%)	41.0± 0.5	40.5± 0.4	37.5± 0.2	32.7± 0.9	42.5± 5.7	37.0± 3.0
P+TG - Best C100 Error (%)	**38.3± 1.1**	**39.2± 0.9**	**33.2± 1.4**	**32.2± 0.8**	**37.6± 1.2**	**33.0± 2.4**
Performance Improvement (%)	2.7	1.3	4.3	0.5	4.9	4

network initial filter weight sampling. Figure 4 shows that the teacher guided search (P+TG) leads to finding network architectures that were on par with performance guided search (P) throughout the search runs while being $10\times$ more efficient.

4.3. Teacher Guided Search in the Space of Convolutional Cells

To compare our approach with recent work on architecture search, we performed a search experiment with P+TG score on the space of convolutional cells [45, 28]. One advantage of this search space compared to those in section 4.2 is that convolutional cells are transferable across datasets. After a cell structure is sampled, the full architecture is constructed by stacking the same cell multiple times with a predefined structure (see supplementary material). While both RL and TPE search methods led to similar outcomes in our experiments in section 4.1, average TPE results were slightly higher for both experiments. Hence, we chose to conduct the search experiment in this section using TPE algorithm with the same setup as in section 4.1 using CIFAR100 with 1000 samples.

For each sample architecture, we computed RDMs for each cell's output. Considering that we had $N = 2$ cell repetitions in each block during search, we ended up with 8 RDMs in each sampled cell that were compared with 3 precomputed RDMs from the teacher network (24 comparisons over validation set of 5000 images). Due to the imperfect correlation between the *premature* and *mature* performances, doing a small post-search reranking step increases the chance of finding slightly better cell structures. We chose the top 10 discovered cells and trained them for 300 epochs on the training set (45k samples) and evaluated on the validation set (5k samples). Cell structure with the highest validation performance was then fully trained on the complete training set (50k samples) for 600 epochs similar to [45] and evaluated on the test set.

We compared our best found cell structure with those found using NAS [45] and PNAS [28] methods on CIFAR-10, CIFAR-100, and Imagenet datasets (Tables 2 and 3).

To rule out any differences in performance that might have originated from differences in training procedure, we used the same training pipeline to train our proposed network (SAGENet) as well as the as well as the two baselines.

With regard to compactness, SAGENet had more parameters and FLOPS compared to NASNet and PNASNet due mostly to symmetric 7×1 and 1×7 convolutions. But we had not considered any costs associated with the number of parameters or the number of FLOPS when conducting the search experiments. For this reason, we also considered another version of SAGENet in which we replaced the symmetric convolutions with "7×7 separable" convolutions (SAGENet-sep). SAGENet-sep had half the number of parameters and FLOPS compared to SAGENet and slightly higher error rates. To compare the cost and efficiency of different search procedures we adopted the same measures as in [28]. Total cost of search was computed as the total number of examples that were processed with SGD throughout the search procedure. This includes M_1 sampled cell structures that were trained with E_1 examples during the search and M_2 top cells trained on E_2 examples post-search to find the top performing cell structure. The total cost was then calculated as $M_1 E_1 + M_2 E_2$.

In sum, we find that while SAGENet performed on par to both NAS and PNAS top networks on C10, C100, and Imagenet, the cost of search was about 100 and 4.5 times less than NASNet and PNASNet respectively (Table 2). Interestingly, at *mature* state our top architecture performed better than the teacher network (ResNet) on C10 and C100 datasets (96.34% and 82.58% on C10 and C100 for TG-SAGE as compared to 94.75% and 75.89% for the ResNet).

4.4. Using Cortical Measurements as the Teacher Network

In the absence of an already high performing teacher network, the utility of TG-SAGE seems unclear (why would one need this method if one already has a high-performing network implemented on a computer?). But what if one does not have that computer implementation, while has partial access to the internal activations of a high performing
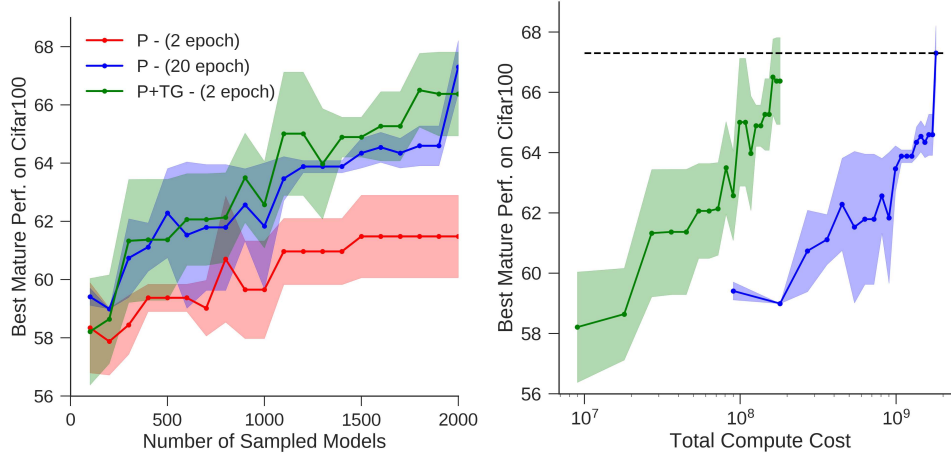
Figure 4. Effect of different surrogate measures on architecture search performance. (left) shows the average C100 performance of the best network architectures found during different stages of three runs of RL search in each case (see text). (right) same as the plot on left but displayed with respect to the total computational cost invested (number of training images × number of epochs × number of samples).

Table 2. Performance of discovered cells on CIFAR10 and CIFAR100 datasets. *indicates error rates from retraining the network using the same training pipeline on 2-GPUs. B: Number of operation blocks in each cell. N: number of cell repetitions in each network block. F: number of filters in the first cell. † estimated GPU days.

Network	# Params	C10 Error	C100 Error	M_1	E_1	M_2	E_2	Cost (Examples)	Cost (GPU days)
AmoebaNet-A [36]	3.2M	3.34	-	20000	1.13M	100	27M	25.2B	(813)
NASNet-A [45]	3.3M	3.41 (3.72*)	17.88*	20000	0.9M	250	13.5M	21.4-29.3B	(690)
PNASNet-5 [28]	3.2M	3.41 (4.06*)	19.26*	1160	0.9M	0	0	1.0B	(32)
ENAS [31]	4.6M	3.54	19.43	310	50k	0	0	15.5M	0.5
GDAS (FRC) [42]	2.5M	3.75	19.09	-	-	-	-	-	1
ASNG + cutout [1]	3.9M	2.83	-	-	-	-	-	-	0.11
DARTS + cutout [29]	3.4M	2.83	-	-	-	-	-	-	4
IRLAS + cutout [17]	3.4M	2.71	-	-	-	-	-	-	-
SAGENet	6.0M	3.66	**17.42**	1000	90K	10	13.5M	225M	(7)
SAGENet-sep	**2.7M**	3.88	17.51						

network? One such network is the primate ventral visual system – it is both high performing in object categorization tasks and is partially observable through electrophysiological recording tools. To test the utility of this idea, we conducted an additional experiment in which we used neural spiking measurements from macaque ventral visual cortex to guide the architecture search.

To facilitate the comparison of representations between the brain's ventral stream and CNNs, we needed a fixed set of inputs that could be shown to both CNNs and the monkeys. For this purpose, we used a set of 5760 images that contained 3D rendered objects placed on uncorrelated natural backgrounds and were designed to include large variations in position, size, and pose of the objects (see supplementary material). We used previously published neural measurements from 296 neural sites in two macaque monkeys in response to these images [43, 30]. These neural responses were measured from three anatomical regions along

the ventral visual pathway (V4, posterior-inferior temporal (p-IT), and anterior inferior temporal (a-IT) cortex) in each monkey – a series of cortical regions in the primate brain that underlie visual object recognition. To allow the candidate networks to be more comparable to the brain measurements, we conducted the experiment on the Imagenet dataset and trained each candidate network for $1/5$ epoch using images of size 64×64. We used the same setup as in section 4.3 but with three RDMs generated from our neural measurements in each area (i.e. V4, p-IT, a-IT). We held out 50,000 of the images from the original Imagenet training set as the validation set that was used to evaluate the premature performance for the candidate networks. To further speed up the search, we removed the first 2 reduction cells in the architecture during the search. Similar to experiments in previous sections, we used $\alpha = 1$ to weigh the RDM similarities compared to the performance in assigning scores to each candidate network. After running the

Table 3. Performance of discovered cells on Imagenet dataset in mobile settings (i.e. number of parameters $\sim 5.5M$ and number of FLOPS<1.5B). Hyperparameters B, N, and F are selected so the network contains approximately 5.5M parametesrs and less than 1.5B FLOPS. *indicates error rates from training all networks using the same training pipeline on 2-GPUs.

Network	B	N	F	# Params (M)	FLOPS (B)	Top-1 Err*	Top-5 Err*
NASNet-A	5	4	44	5.3	1.16	31.07	11.41
PNASNet-5	5	3	56	5.4	1.30	**29.92**	**10.63**
SAGENet	5	4	48	9.7	2.15	31.81	11.79
SAGENet-sep				4.9	1.03	31.9	11.99

Table 4. Comparison of best networks found with performance-guided and neurally guided architecture searches in the space of convolutional cells on Imagenet.

Network	B	N	F	# Params (M)	FLOPS (B)	Top-1 Err	Top-5 Err
P-imagenet	5	4	40	5.5	1.26	34.4	13.5
SAGENet-neuro	5	3	40	5.6	1.35	**32.54**	**12.26**

architecture search for 1000 samples, we picked the top 10 networks and fully trained them on Imagenet for 40 epochs and picked the network with highest validation accuracy. We then trained this network on the full Imagenet training set and evaluated its performance on the test set. As a baseline, we also performed a similar search but using only the performance metric to guide the search.

We found that the best discovered network using the combined P+TG metric (SAGENet-neuro) had a significantly lower top-1 error (32.54%) than the best network derived from performance-guided search (34.4%; P-imagenet; see Table 4). This suggests that the approach has potential merit. However, when searching on CIFAR-100 dataset, the best model found by using the partially observed internal representations of the primate brain teacher network (SAGENet-neuro) did not perform as well as the model found by using the fully observed internal representations of the ResNet teacher network. One critical factor that might have affected the quality of the best discovered model was the amount of per-sample training done during the search (this was limited to 2000 steps (1/5epoch) in our experiment). Naturally, allowing more training before evaluation would potentially result in a more accurate prediction of mature performance and discovering a higher performing model. Another important factor was the partially observations of the brain – neural recordings for constructing a teacher RDM would likely be further improved with larger population of neural responses measured in response to more stimuli. Nevertheless, the teacher representations constructed from only a few hundred primate neural sites was already informative enough to produce improved guidance for architecture search.

5. Discussion and Future Directions

We here demonstrate that, when the internal neural representations of a high performing teacher neural network are partially observable (such as the brain's neural network), that knowledge can substantially accelerate the discovery of high performing artificial networks. We propose a new method to accomplish that acceleration (TG-SAGE) and demonstrate its utility using an existing state-of-the-art computerized network as the teacher (ResNet) and its potential using a partially-observed biological network as the teacher (primate ventral visual stream). Essentially, TG-SAGE jointly maximizes a model's *premature* performance and its internal representational similarity to those of a partially observable teacher network. With the architecture space and search settings tested here, we report a computational efficiency gain of $\sim 10\times$ in discovering CNNs for performance on visual categorization. This gain in search efficiency (reduced computational resource budget with similar categorization performance) was achieved without any additional constraints on the search space as in alternative search methods like ENAS [31] or DARTS [29]. We empirically demonstrated this by performing searches in several CNN architectural spaces.

Could this approach be applied at scale using high performing biological systems? We here showed how limited measurements from the brain (neural population patterns of responses to many images) could be formulated as teacher constraints to accelerate the search for higher performing networks. It remains to be seen if larger scale neural measurements – which are obtainable in the near future – could achieve even better acceleration.

References

[1] Youhei Akimoto, Shinichi Shirakawa, Nozomu Yoshinari, Kento Uchida, Shota Saito, and Kouhei Nishida. Adaptive Stochastic Natural Gradient Method for One-Shot Neural Architecture Search. In *ICML*, 2019. 2, 7

[2] Luke Arend, Yena Han, Martin Schrimpf, Pouya Bashivan, Kohitij Kar, Tomaso Poggio, James J DiCarlo, and Xavier Boix. Single units in a deep neural network functionally correspond with neurons in the brain: preliminary results. Technical report, Center for Brains, Minds and Machines (CBMM), 2018. 3

[3] Jimmy Ba and Rich Caruana. Do deep nets really need to be deep? In *Advances in neural information processing systems*, pages 2654–2662, 2014. 2

[4] Bowen Baker, Otkrist Gupta, Nikhil Naik, and Ramesh Raskar. Designing neural network architectures using reinforcement learning. *arXiv preprint arXiv:1611.02167*, 2016. 2

[5] Bowen Baker, Otkrist Gupta, Ramesh Raskar, and Nikhil Naik. Practical neural network performance prediction for early stopping. *arXiv preprint arXiv:1705.10823*, 2017. 2

[6] Pouya Bashivan, Kohitij Kar, and James J DiCarlo. Neural population control via deep image synthesis. *Science*, 364(6439):eaav9436, 2019. 3

[7] James Bergstra, Remi Bardenet, Yoshua Bengio, and Balazs Kegl. Algorithms for Hyper-Parameter Optimization. pages 1–9, 2011. 5

[8] J. Bergstra, D. Yamins, and D. D. Cox. Making a Science of Model Search. pages 1–11, 2012. 1

[9] Nathaniel Blanchard, Jeffery Kinnison, Brandon Richard-Webster, Pouya Bashivan, and Walter J Scheirer. A neurobiological cross-domain evaluation metric for predictive coding networks. In *Conference on Computer Vision and Pattern Recognition*, 2019. 3

[10] Andrew Brock, Theodore Lim, J. M. Ritchie, and Nick Weston. SMASH: One-Shot Model Architecture Search through HyperNetworks. 2017. 2

[11] Santiago A Cadena, George H Denfield, Edgar Y Walker, Leon A Gatys, Andreas S Tolias, Matthias Bethge, and Alexander S Ecker. Deep convolutional models improve predictions of macaque V1 responses to natural images Author summary. *Plos*, pages 1–28, 2017. 3

[12] Charles F. Cadieu, Ha Hong, Daniel L K Yamins, Nicolas Pinto, Diego Ardila, Ethan A. Solomon, Najib J. Majaj, and James J. DiCarlo. Deep Neural Networks Rival the Representation of Primate IT Cortex for Core Visual Object Recognition. *PLoS Computational Biology*, 10(12), 2014. 3

[13] Joao Carreira, Viorica Patraucean, Laurent Mazare, Andrew Zisserman, and Simon Osindero. Massively Parallel Video Networks. In *ECCV*, 2018. 2

[14] Tobias Domhan, Jost Tobias Springenberg, and Frank Hutter. Speeding up automatic hyperparameter optimization of deep neural networks by extrapolation of learning curves. 15:3460–8, 2015. 2

[15] Ruth C. Fong, Walter J. Scheirer, and David D. Cox. Using human brain activity to guide machine learning. *Scientific Reports*, 8(1):1–10, 2018. 3

[16] Ian J. Goodfellow, Jonathon Shlens, and Christian Szegedy. Explaining and Harnessing Adversarial Examples. pages 1–11, 2014. 3

[17] Minghao Guo, Zhao Zhong, Wei Wu, Dahua Lin, and Junjie Yan. IRLAS: Inverse Reinforcement Learning for Architecture Search. In *CVPR*, 2018. 2, 7

[18] David Ha, Andrew Dai, and Quoc V. Le. HyperNetworks. 2016. 2

[19] Kaiming He, Xiangyu Zhang, Shaoqing Ren, and Jian Sun. Deep Residual Learning for Image Recognition. *Arxiv.Org*, 7(3):171–180, 2015. 1, 4

[20] Geoffrey Hinton, Oriol Vinyals, and Jeff Dean. Distilling the knowledge in a neural network. *arXiv preprint arXiv:1503.02531*, 2015. 2

[21] Gao Huang, Zhuang Liu, Laurens van der Maaten, and Kilian Q. Weinberger. Densely Connected Convolutional Networks. 2016. 1

[22] Kamila M. Jozwik, Nikolaus Kriegeskorte, Katherine R. Storrs, and Marieke Mur. Deep convolutional neural networks outperform feature-based but not categorical models in explaining object similarity judgments. *Frontiers in Psychology*, 8(OCT):1726, 2017. 3

[23] Alexander JE Kell and Josh H. McDermott. Deep neural network models of sensory systems: windows onto the role of task constraints. *Current Opinion in Neurobiology*, 55:121–132, 2019. 3

[24] Nikolaus Kriegeskorte, Marieke Mur, and Peter a. Bandettini. Representational similarity analysis - connecting the branches of systems neuroscience. *Frontiers in systems neuroscience*, 2(November), 2008. 3

[25] Alex Krizhevsky, Ilya Sutskever, and Geoffrey E Hinton. ImageNet Classification with Deep Convolutional Neural Networks. *Advances In Neural Information Processing Systems*, pages 1–9, 2012. 1

[26] Jonas Kubilius, Stefania Bracci, and Hans P. Op de Beeck. Deep Neural Networks as a Computational Model for Human Shape Sensitivity. *PLoS Computational Biology*, 12(4):1–26, 2016. 3

[27] Lisha Li, Kevin Jamieson, Giulia DeSalvo, Afshin Rostamizadeh, and Ameet Talwalkar. Hyperband: A novel bandit-based approach to hyperparameter optimization. *The Journal of Machine Learning Research*, 18(1):6765–6816, 2017. 2

[28] Chenxi Liu, Barret Zoph, Jonathon Shlens, Wei Hua, Li-Jia Li, Li Fei-Fei, Alan Yuille, Jonathan Huang, and Kevin Murphy. Progressive Neural Architecture Search. 2017. 1, 6, 7

[29] Hanxiao Liu, Karen Simonyan, and Yiming Yang. DARTS: Differentiable Architecture Search. 2018. 2, 7, 8

[30] N. J. Majaj, H. Hong, E. A. Solomon, and J. J. DiCarlo. Simple Learned Weighted Sums of Inferior Temporal Neuronal Firing Rates Accurately Predict Human Core Object Recognition Performance. *Journal of Neuroscience*, 35(39):13402–13418, 2015. 7

[31] Hieu Pham, Melody Y. Guan, Barret Zoph, Quoc V. Le, and Jeff Dean. Efficient Neural Architecture Search via Parameters Sharing. 2018. 2, 7, 8

[32] Nicolas Pinto, David Doukhan, James J DiCarlo, and David D Cox. A high-throughput screening approach to discovering good forms of biologically inspired visual representation. *PLoS computational biology*, 5(11):e1000579, 2009. 1, 5

[33] Maithra Raghu, Justin Gilmer, Jason Yosinski, and Jascha Sohl-Dickstein. SVCCA: Singular Vector Canonical Correlation Analysis for Deep Learning Dynamics and Interpretability. 2017. 4

[34] Rishi Rajalingham, Elias B Issa, Pouya Bashivan, Kohitij Kar, Kailyn Schmidt, and James J Dicarlo. Large-scale, high-resolution comparison of the core visual object recognition behavior of humans, monkeys, and state-of-the-art deep artificial neural networks. *The Journal of neuroscience*, 014970(33):240614, 2018. 3

[35] R. Rajalingham, K. Schmidt, and J. J. DiCarlo. Comparison of Object Recognition Behavior in Human and Monkey. *Journal of Neuroscience*, 35(35):12127–12136, 2015. 3

[36] Esteban Real, Alok Aggarwal, Yanping Huang, and Quoc V Le. Regularized Evolution for Image Classifier Architecture Search. (2017), 2018. 1, 2, 7

[37] Esteban Real, Sherry Moore, Andrew Selle, Saurabh Saxena, Yutaka Leon Suematsu, Quoc Le, and Alex Kurakin. Large-Scale Evolution of Image Classifiers. 2016. 1, 2

[38] Adriana Romero, Nicolas Ballas, Samira Ebrahimi Kahou, Antoine Chassang, Carlo Gatta, and Yoshua Bengio. FitNets: Hints for Thin Deep Nets. pages 1–13, 2014. 2

[39] Martin Schrimpf, Jonas Kubilius, Ha Hong, Najib J Majaj, Rishi Rajalingham, Elias B Issa, and Kohitij Kar. Brain-Score : Which Artificial Neural Network for Object Recognition is most Brain-Like ? pages 1–9, 2018. 2

[40] Ian H Stevenson and Konrad P Kording. How advances in neural recording affect data analysis. *Nature neuroscience*, 14(2):139, 2011. 2

[41] Christian Szegedy, Vincent Vanhoucke, Jonathon Shlens, and Zbigniew Wojna. Rethinking the Inception Architecture for Computer Vision. 2014. 1

[42] Yi Yang Xuanyi Dong. Searching for A Robust Neural Architecture in Four GPU Hours — Xuanyi Dong. *Computer Vision and Pattern Recognition 2019*, pages 1761–1770, 2019. 2, 7

[43] D. L. K. Yamins, H. Hong, C. F. Cadieu, E. A. Solomon, D. Seibert, and J. J. DiCarlo. Performance-optimized hierarchical models predict neural responses in higher visual cortex. *Proceedings of the National Academy of Sciences*, 111(23):8619–8624, 2014. 2, 3, 7

[44] Barret Zoph and Quoc V Le. Neural architecture Search With reinforcement learning. *ICLR*, 2017. 1, 2, 5

[45] Barret Zoph, Vijay Vasudevan, Jonathon Shlens, and Quoc V. Le. Learning Transferable Architectures for Scalable Image Recognition. 10, 2017. 1, 2, 6, 7